Egyptian Journal of Chemistry

http://ejchem.journals.ekb.eg/

Effect of Some Aliphatic Amines as Corrosion Inhibitors for AZ91 alloy

Sh. Bahaa, O.R.M. Khalifa, A.K. Kassab, M. M. Esmail , S. Y. Ahmed*

Chemistry department, Faculty of Girls for Arts, Science and Education, Ain shams University, Cairo, Egypt

Abstract

The corrosion behaviour of AZ91 alloy was investigated in 0.1M hydrochloric acid solution at different temperatures 20-50○C. The study was done by weight loss technique and electrochemical method, using Tafel polarization technique. The additive concentration increases the inhibition effectiveness. The results show that the protection efficiency P% followed the sequence ethylenediamine (EDA) > diethylamine (DEA) > ethylamine (EA). The influence of temperature on the corrosion behaviour of AZ91 alloy in 0.1M HCl solution was studied between 20○C and 50○C both with and without inhibitors. The inhibition efficiencies obtained from the two employed methods (weight loss technique and potentiodynamic polarization technique) are nearly closed. From the obtained data, it was found that, the inhibition efficiency increases with increasing the inhibitor concentration until the optimum one. Adsorption of the inhibitors on AZ91 alloy surface was found to obey Langmuir's adsorption isotherm. SEM examination of AZ91 alloy surface revealed that these inhibitors prevented AZ91 from corrosion by adsorption on its surface to form a protective film, which acts as barrier to aggressive agents.

Keywords: AZ91 alloy; aliphatic amine; Inhibition; Corrosive media.

1. Introduction

Magnesium-aluminum alloys have drawn increased interest in the aerospace, automotive, and electronic industries because of their ultralightness, good castability, strong specific strength, and low energy consumption [1–6]. Commercial magnesium materials with high strength and low cost include Mg-Al-Zn alloys. Thanks to recent advancements in rolling technology that allow for the production of wide-scale Mg-Al-Zn sheets with enhanced mechanical properties, Mg-Al-Zn alloys are now more productive as suitable components for applications requiring a high weight tolerance [7]. AZ91 is a magnesium alloy that is most frequently used and is available for purchase. It exhibits a good balance of ductility, mechanical strength, and castability [8,9]. It is also a popular lightweight material alloy, particularly in the biomedical and automotive industries, which seek to produce lightweight vehicles [10,11]. To encourage the broader use of magnesium alloy, an appropriate treatment can improve its corrosion resistance, which has significant practical implications. One of the most effective methods for slowing the progression of metal corrosion is to introduce a corrosion inhibitor into the corrosive solution in small concentrations [12–14]. Numerous researchers have discussed how organic inhibitors affect how magnesium alloy corrodes in hydrochloric acid [15–22]. Typically, these substances include heteroatoms like O, S, N, and P that serve as coordination sites for adsorption on the surface of the metal. A surface-protective layer is created by adsorption. Amines and their derivatives, which have a variety of molecular structures, are among the many known corrosion inhibitors and differ in their ability to inhibit corrosion in certain ways [23–30]. In organic ammonia compounds known as amines, one or more hydrogen atoms are swapped out for variously sized and numbered hydrocarbon chains. The subclass of compounds is determined by the number of hydrocarbon chains joined to the N atom. Three different types of amines can be identified by the presence of the -NH2, -NHR, and -NR1R2 groups, which are hydrocarbon chains with one, two, or three links to the N atom [31]. The effects of hexamethylenetetramine on AZ31B alloys were studied, and their protection efficiency was found to be 94.57 % [31]. The corrosion inhibition efficiency of triethanolamine in 3.5 wt% NaCl solution with AZ91D magnesium alloy has been investigated [32]. In a 3.5% NaCl environment, a butylamine-modified GO material was developed as an anticorrosion finish for magnesium alloys [33]. However, only a few studies on the anticorrosion properties of amines on magnesium alloys have been published. Therefore, we investigated the possibility of AZ91 alloy in 0.1M HCl inhibition by some aliphatic amines**.**

2. Experimental

AZ91 alloy samples are circular discs with an area of 10.2 cm2. The AZ91 alloy used in this study has the following analysis Zn 1.1%, Al 9.05%, Mn 0.27%, Cu 0.019%, Fe 0.02%, and balanced Mg, which provided by the Central Metallurgical Research Institute (CMRDI) .

First, the substrates were mechanically grinded using 800, 2000, and 3000 Si abrasive papers, respectively. The substrate was then cleaned with deionized water, treated with acetone for 10 min to remove any remaining grease, and allowed to air dry. The inhibiting properties of EDA, DEA, and EA were studied using the technique of weight loss with and without inhibitors (1, 0.5, 0.2, and 0.1M) in 0.1 M HCl corrosive media at different temperatures (20, 30, 40 and 50˚C).

The sheets were suspended in 100 ml of a 0.1M solution of HCl with and without various inhibitor concentrations for 30 min. Loss in weight per area in µg/cm2 (Wt.). The equations below were used to determine the percentage of protection effectiveness (P%) and the corrosion rate (V_{corr}) for a range of inhibitor concentrations.

*Corresponding author e-mail: safaa.yhaia@women.asu.edu.eg , (**S. Y. Ahmed**).

Receive Date: 15 May 2024, Revise Date: 07 June 2024, Accept Date: 23 June 2024

DOI: 10.21608/ejchem.2024.290066.9719

$$W_t = \frac{W_0 - W_1}{A} \quad (1)$$

$$V_{corr} = \frac{W_t}{t} \quad (2)$$

$$P\% = \left[1 - \frac{V`corr}{V_{corr}}\right] \times 100 \quad (3)$$

Where w_o is the starting weight in micrograms, w_1 is the weight after being submerged inside the electrolyte, t is the time of immersion (sec.), and V'_{corr} and V_{corr} are the corrosion rates with and without an inhibitor, respectively.

The surface morphology was displayed using a Quanta 250 FEG scanning electron microscope (SEM) from Taiwan. Different samples were examined while being subjected to a 30 kv accelerating voltage. Carbon paste was used to grind the samples before mounting. In each case, the average weight loss between the two measurements was recorded. Potentiodynamic polarization studies were performed on test specimens exposing 1 cm2 of the surface in the range of 0 to -250 mV using a CHI instrument and a scan rate of 0.5 mV/s. A test specimen served as the working electrode in the cell, the reference electrode was an Ag/AgCl electrode, and the counter electrode was a Pt electrode.

2.Results and discussion

a.Corrosion rate and protection efficiency

The average rate of corrosion (V_{corr}) of AZ91 expressed as ($\mu g.cm^{-2}.sec^{-1}$) it is displayed in Fig.1 as a function of the logarithmic concentrations of EDA, DEA, and EA in a 0.1 M solution of HCl at 30 °C. They show how the corrosiveness of the acid is lowered by the organic inhibitors that are added. The amount of inhibitors present influences the rate at which AZ91 corrodes. Their behavior is determined by the nature of the substituent

The variation in the protection effectiveness of AZ91 as a function of the logarithmic concentrations of EDA, DEA, and EA in a 0.1 M solution of HCl at 30 °C is shown in Fig. 2. With increasing inhibitor concentrations, the protection effectiveness increases.

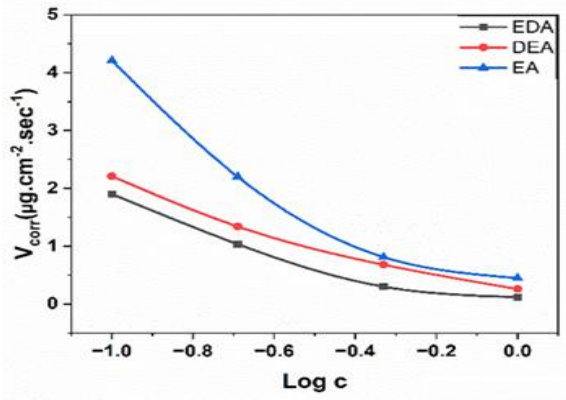

Fig. 1. Effect of EDA, DEA, and EA concentrations on AZ91 corrosion rates in 0.1M HCl solution

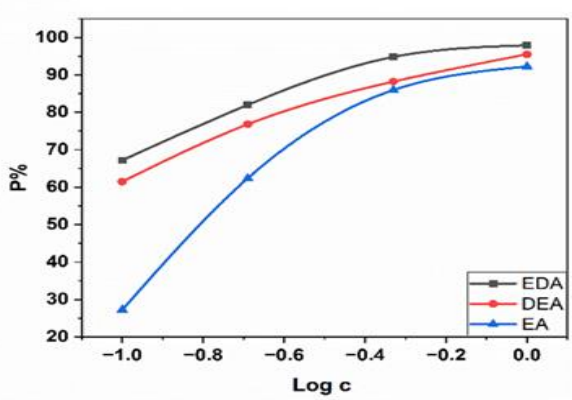

Fig.2. Relationship between percentage protection and log inhibitor concentrations of EDA, DEA, and EA at 30°C in 0.1M HCl.

Moreover, the protection efficiency increases from EDA> DEA>EA (as shown in Table 1).

Table 1. The effectiveness of various inhibitor's protection in a 0.1M HCl solution was calculated from equation (1) at 30˚C.

Conc. of the inhibitor	EDA		DEA		EA	
	V_{corr} ($\mu g.cm^{-2}.sec^{-1}$)	P%	V_{corr} ($\mu g.cm^{-2}.sec^{-1}$)	P%	V_{corr} ($\mu g.cm^{-2}.sec^{-1}$)	P%
1 M	0.12	97.90	0.26	95.50	0.47	92.24
0.5 M	0.30	94.80	0.68	88.20	0.81	85.65
0.2 M	1.035	82	1.34	76.81	2.20	62.39
0.1 M	1.90	67.20	2.21	61.5	4.21	27.24

As a function of the logarithmic concentration of EDA, DEA, and EA at various temperatures, Fig. 3 shows the variation in the corrosion rate of AZ91. The corrosion rate increases by the increase of the temperature 50 > 40 > 30 > 20°C.

Figure 4 , illustrates how the concentrations of EDA, DEA, and EA affect the effectiveness of AZ91 protection at various temperatures. For EDA, DEA, and EA, the same behavior has been noticed. In general, as temperatures decrease, the protection effectiveness increases. This implies that these substances are adsorbed onto the surface of the AZ91 physically.

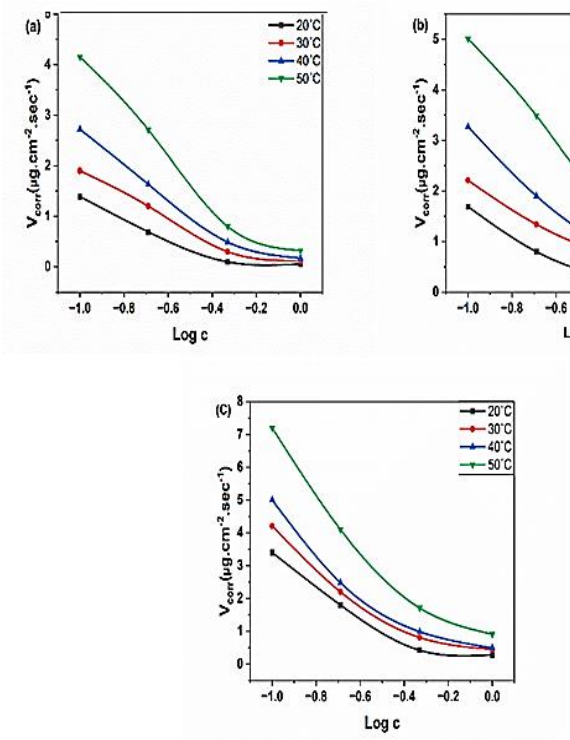

Fig. 3. Effect of (a) EDA, (b) DEA, and (c) EA concentrations on the rate of AZ91 corrosion in 0.1M HCl solution at various temperatures.

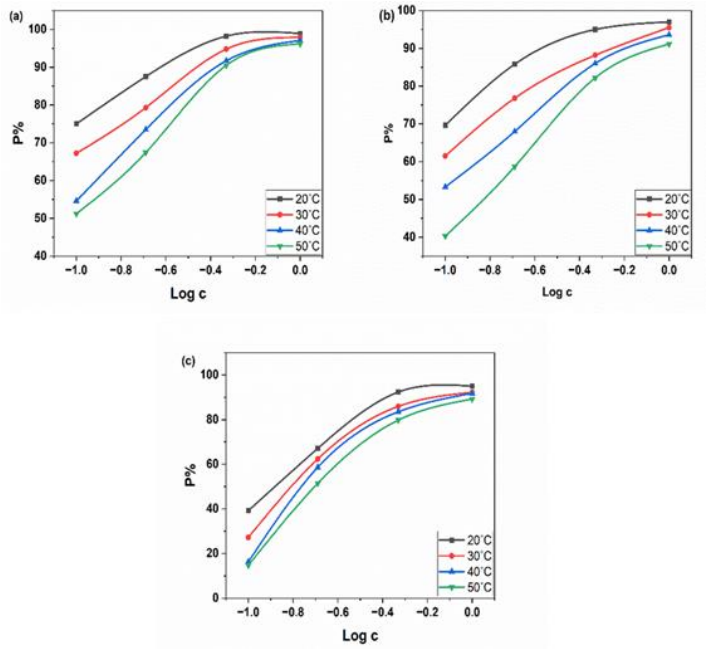

Fig.4. Effect of (a) EDA, (b) DEA, and (c) EA concentrations on the effectiveness of AZ91 protection in a 0.1M HCl solution at various temperatures.

3.2. Adsorption isotherm

It has been reported that the adsorption of an organic compound onto the surface of the metal is dependent on the physicochemical properties of the inhibitor's molecule, such as length, steric factors, functional groups and electron density (i.e., charge distribution) at the donor atoms and π orbital character of donating electrons, as well as the nature of the subtrating metal and the manner in which an organic molecule interacts with a metallic surface [31,34–36].

The adsorption behavior at 30 °C was studied to better understand the electrochemical process on the metal surface. From the weight loss measurements, the degree of surface coverage (θ) at various concentrations in an acidic medium was calculated using equation (4).

$$\theta = 1 - \frac{V`_{corr}}{V_{corr}} \qquad (4)$$

The best adsorption isotherm was chosen after graphic testing of the data related to the extent of surface coverage (θ).
Fig. 5, plotting c/θ versus the change in inhibitor concentration to AZ91 in 0.1 M HCl, shows a straight line, indicating that the adsorption of these inhibitors is properly described by the Langmuir adsorption isotherm [37]. Equation (5) describes these isotherms [38].

$$\frac{c}{\theta} = \frac{1}{k} + \mathrm{c} \qquad (5)$$

$$k = \frac{1}{55.5}\ exp\ \frac{\Delta G^{\circ}}{RT} \qquad (6)$$

where is the standard free energy of adsorption (ΔG˚), C is the concentration of the inhibitor, and k is the adsorption constant [39–41]. Table 2 displays the adsorption reaction`s calculated k and ΔG˚ values for AZ91

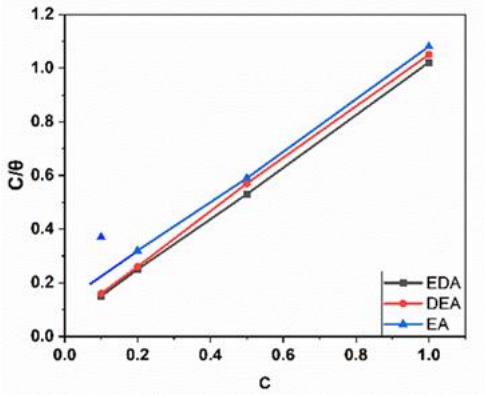

Fig.5. EDA, DEA, and EA compounds adsorb on the surface of the AZ91 alloy in 0.1M HCl at 30°C according to the Langmuir adsorption isotherm.

The fact that the standard free energy of adsorption has a negative value indicates that these inhibitors spontaneously adsorb on the AZ91 alloy. This means that the previously mentioned physical adsorption is what gives these substances their inhibitory effects.

3.2.1. Activation energy

Using the Arrhenius equation as a guide

$$Ln\ k = Ln\ A + \frac{-E_a}{RT} \qquad (7)$$

where A is the pre-exponential Arrhenius parameter, Ea is the apparent activation energy, and K is the rate of the metal dissolution reaction [42], Equation (8) establishes a direct relationship between the apparent activation energy Ea and the corrosion rate (V_{corr}).

$$Ln\ V_{corr} = Ln\ A + \frac{-E_a}{RT} \qquad (8)$$

The corrosion rate of the AZ91 alloy in a 0.1 M solution of HCl is plotted logarithmically as a function of (1/T) in the uninhibited and inhibited solutions, respectively, in Fig. 6.
For the inhibitor-free solution, the energy of activation, evaluated from this graph, was found to be equal to 4.15 j.mol^{-1}. K^{-1} for AZ91. In the presence of either of the studied inhibitors, the activation energy increases. The 1M concentrations of EDA, DEA, and EA are 19.09, 16.60, 12.45 j.mol^{-1}.K^{-1} for AZ91, which agree with previously published data [43]. This value is also the order of activation encountered for a physical mechanism.

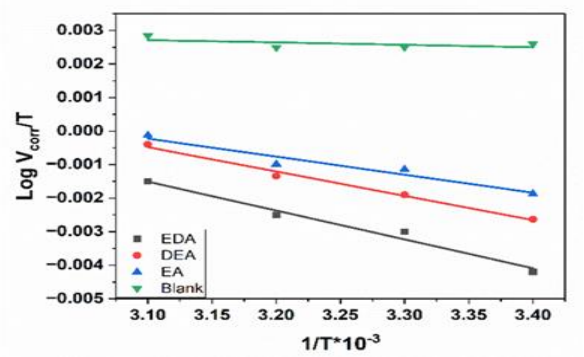

Fig.6. Logarithmic plot of the corrosion rate of the AZ91 alloy as a function of (1/T) in both uninhibited and inhibited solutions.

The transition state equation (9) was used to determine the Enthalpy and entropy of activation, ΔH°, and ΔS°, respectively.

$$V_{corr} = \frac{R}{NH}\left[exp\frac{\Delta S^{\circ}}{R}\right]\left[exp\frac{-\Delta H^{\circ}}{RT}\right] \qquad (9)$$

Straight lines were obtained for AZ91 by plotting Log (V_{corr}/T) vs. 1/T at 0.1 M HCl of the studied inhibitors, as shown in Fig. 7. Straight line slopes and intercepts can be applied to calculate the values of ΔH° and ΔS°, respectively, as shown in Table 2

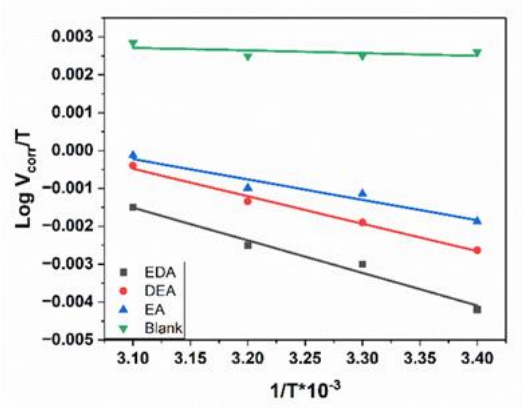

Fig.7. AZ91 alloy in 0.1M HCl, log (V_{corr}/T) vs. (1/T) on both uninhibited and inhibited solutions of EDA, DEA, and EA.

Table 2. Thermodynamic activation parameters for the dissolution of AZ91 in a 0.1 M solution of HCl containing 1M of various inhibitors.

	K (L mol^{-1})	ΔH (KJ mol^{-1})	-ΔG (KJ mol^{-1})	-ΔS (J mol^{-1}K^{-1})
EDA	7500	20.10	32.5	173.6
DEA	6250	15.90	32.40	159.41
EA	2500	12.50	29.88	139.87

3.3. Scanning electron microscopy

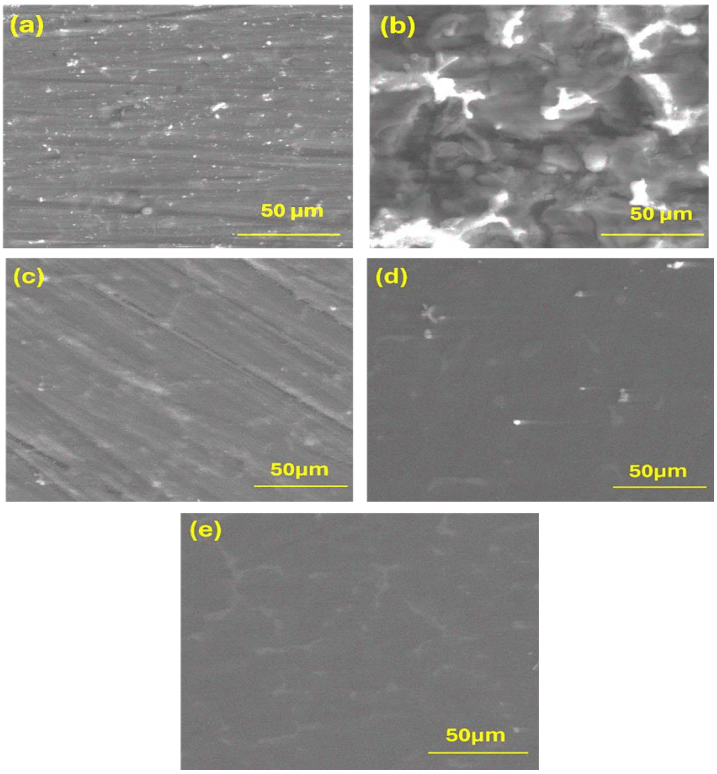

Fig.8. Scanning electron microscope images of (a) AZ91 alloy, (b) AZ91 alloy in 0.1M HCl, (c) AZ91 alloy in the presence of EA, (d) DEA, and (e) EDA.

Fig. 8 shows the morphology of (a) AZ91 alloy, (b) AZ91 alloy in 0.1M solution of HCl, (c) the existence of EA, (d) the existence of DEA, and (e) the existence of EDA. Before dipping in corrosive media with and without the inhibitors EDA, DEA, and EA.

It is clear that the corrosion attack was more pronounced in absence of additives, while by the addition of different inhibitors the film formed on AZ91 surface becomes more protective. The protective film is more pronounced for EDA > DEA > EA.

3.4. Potentiodynamic polarization measurements

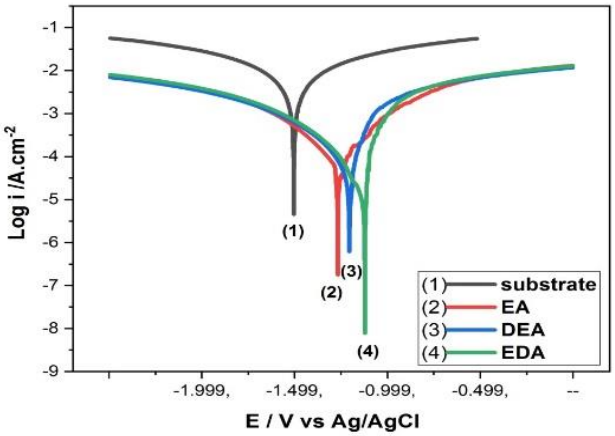

Fig. 9. AZ91 alloy potentiodynamic polarization curves in a 0.1 M solution of HCl in the presence and absence of the tested inhibitors.

Fig. 9 displays the AZ91 alloy's potentiodynamic polarization curves in a 0.1 M solution of HCl both in the absence and presence of the tested inhibitors being studied. Table 3 shows the respective kinetic parameters, including corrosion current density (I_{corr}), corrosion potential (E_{corr}).

The corrosion potential (E_{corr}) and corrosion current density (I_{corr}) were calculated by fitting the plots using the EC-lab software. The fitting parameters are listed in Table 3. Our amine derivative inhibitor can be categorized as a mixed-type inhibitor because of the shift of cathodic and anodic branches of Tafel lines with reduced current densities compared with the sample in the absence of inhibitor. The adsorption of organic species on the electrode surface may lead to a large (more than 1 V) negative or positive shift of the potential of zero charge. The presence of the three studied inhibitors resulted in a positive corrosion potential. The inhibition efficiency, η (%), was calculated from Eq. (11) and the results are listed in Table 3. I_{corr} decreases with the presence of inhibitors, and the protection efficiency of EDA has higher protection efficiency, which agree with the weight loss technique.

$$\eta(\%) = \frac{i^0_{corr} - i_{corr}}{i^0_{corr}} \times 100 \qquad (10)$$

Table 3. Electrochemical data from potentiodynamic polarization curves for the AZ91 alloy in a 0.1 M solution of HCl in both uninhibited and inhibited solutions.

	I_{corr} (μA)	E_{corr} (mV)	η (%)
EDA	25	-1222	98.42
DEA	100	-1248	93.68
EA	125	-1267	92.10
Blank	1584	-1494	--

Conclusions

The current research has conclusively shown that aliphatic amines inhibit corrosion of the AZ91 alloy in 0.1 M HCl. Additive concentration enhances the inhibition efficiency. The calculation of protection efficiency (P%) by weight loss follows the sequences 97.9, 95.5, and 92.24 for EDA, DEA, and EA, respectively. The effectiveness of inhibition decreases with increasing temperature and increases with inhibitor concentration. The adsorption of the inhibitor under investigation is described by the Langmuir adsorption isotherm and shows physical adsorption. The cathodic and anodic branches of the Tafel lines shifted in the noble direction and had lower current densities than the sample bath without the inhibitor, Thus, our amine derivative inhibitors can be classified as mixed-type inhibitors. The morphology of the inhibitors shows that these substances have the capacity to adsorb on metal surfaces, blocking the active sites and reducing the rate of corrosion.

Conflicts of interest

"There are no conflicts to declare".

Acknowledgments

The Faculty of Women for Arts, Science, and Education at Ain Shams University provided the authors with research support, which they gratefully acknowledge.

References

[1] Li H, Fan M, Wang K, Xu G, Jiang H, Wang Q, et al. TiCN nanoparticle-induced corrosion inhibition mechanisms of AZ91 alloy. Corrosion Science 2022;198:110109. https://doi.org/10.1016/j. corsci.2022.110109.

[2] Joost WJ, Krajewski PE. Towards magnesium alloys for high-volume automotive applications. Scripta Materialia 2017;128:107–12. https://doi.org/10.1016/j.scriptamat.2016.07.035.

[3] Omiyale BO, Olugbade TO, Abioye TE, Farayibi PK. Wire arc additive manufacturing of aluminium alloys for aerospace and automotive applications: a review. Materials Science and Technology (United Kingdom) 2022;38:391–408. https://doi.org/10.1080/02670836.2022.2045549.

[4] Tan J, Ramakrishna S. Applications of magnesium and its alloys: A review. Applied Sciences (Switzerland) 2021;11. https://doi.org/10.3390/app11156861.

[5] Lamaka S V., Vaghefinazari B, Mei D, Petrauskas RP, Höche D, Zheludkevich ML. Comprehensive screening of Mg corrosion inhibitors. Corrosion Science 2017;128:224–40. https://doi.org/10.1016/j .corsci.2017.07.011.

[6] Zhang Y, Liu B, Chen S, Xu K. A new idea for industrial safety in magnesium grinding: Suppression of hydrogen generation in wet dust collectors. International Journal of Hydrogen Energy 2022;47:20333–46. https://doi.org/10.1016/j.ijhydene.2022.04.131.

[7] Wei D, Wang J, Liu Y, Wang D, Li S, Wang H. Controllable superhydrophobic surfaces with tunable adhesion on Mg alloys by a simple etching method and its corrosion inhibition performance. Chemical Engineering Journal 2021;404:126444. https://doi.org/10.1016/J.CEJ.2020.126444.

[8] Wei D, Wang J, Liu Y, Wang D, Li S, Wang H. Controllable superhydrophobic surfaces with tunable adhesion on Mg alloys by a simple etching method and its corrosion inhibition performance. Chemical Engineering Journal 2021;404:126444. https://doi.org/10.1016/j.cej.2020.126444.

[9] Asadi P, Givi MKB, Akbari M. Simulation of dynamic recrystallization process during friction stir welding of AZ91 magnesium alloy. International Journal of Advanced Manufacturing Technology 2016;83:301–11. https://doi.org/10.1007/s00170-015-7595-z.

[10] Akbari M, Asadi P, Givi MKB, Zolghadr P. A cellular automaton model for microstructural simulation of friction stir welded AZ91 magnesium alloy. Modelling and Simulation in Materials Science and Engineering 2016;24:35012. https://doi.org/10.1088/0965-0393/24/3/035012.

[11] Ramalingam VV, Ramasamy P, Kovukkal M Das, Myilsamy G. Research and Development in Magnesium Alloys for Industrial and Biomedical Applications: A Review. Metals and Materials International 2020;26:409–30. https://doi.org/10.1007/s12540-019-00346-8.

[12] Ouici HB, Benali O, Harek Y, Larabi L, Hammouti B, Guendouzi A. Inhibition of mild steel corrosion in 5 % HCl solution by 5-(2-hydroxyphenyl)-1,2,4-triazole-3-thione. Research on Chemical Intermediates 2013;39:2777–93. https://doi.org/10.1007/s11164-012-0797-1.

[13] Benali O, Zebida M, Maschke U. Synthesis and inhibition corrosion effect of two thiazole derivatives for carbon steel in 1 M HCl. Journal of the Indian Chemical Society 2021;98:100113. https://doi.org/10.1016 /j.jics.2021.100113.

[14] Štrbák M, Kajánek D, Knap V, Florková Z, Pastorková J, Hadzima B, et al. Effect of Plasma Electrolytic Oxidation on the Short-Term Corrosion Behaviour of AZ91 Magnesium Alloy in Aggressive Chloride Environment. Coatings 2022;12. https://doi.org/10.3390/coatings12050566.

[15] Shang W, Yin ZL, Wen YQ, Wang XF. Corrosion inhibition of polyethylene glycol for magnesium alloy AZ91 at different temperatures. Advanced Materials Research 2014;1015:692–5. https://doi.org/10.4028/www.scientific.net/ AMR.1015.692.

[16] Slavcheva E, Petkova G, Andreev P. Inhibition of corrosion of AZ91 magnesium alloy in ethylene glycol solution in presence of chloride anions. Materials and Corrosion 2005;56:83–7. https://doi.org/10.1002/maco.200403829.

[17] Dang N, Wei YH, Hou LF, Li YG, Guo CL. Investigation of the inhibition effect of the environmentally friendly inhibitor sodium alginate on magnesium alloy in sodium chloride solution. Materials and Corrosion 2015;66:1354–62. https://doi.org/10.1002/maco.201408141.

[18] Xie ZH, Wu L. Corrosion inhibition of layered double hydroxide coating for Mg alloy in acidic corrosive environments. Materials and Corrosion 2020;71:118–24. https://doi.org/10.1002/maco.201910995.

[19] Xavier JR, Beryl JR, Vinodhini SP, Janaki GB. Enhanced Protective and Mechanical Properties of Polypyrrole Coatings Modified by Silane/CoO Nanocomposite on AZ91 Mg Alloy in Chloride Media. Journal of Bio- and Tribo-Corrosion 2021;7:1–17. https://doi.org/10.1007/s40735-021-00479-7.

[20] Atrens A, Shi Z, Mehreen SU, Johnston S, Song GL, Chen X, et al. Review of Mg alloy corrosion rates. Journal of Magnesium and Alloys 2020;8:989–98. https://doi.org/10.1016/j.jma.2020.08.002.

[21] Ali MAA. Inhibition of mild steel corrosion in cooling systems by low-and non-toxic corrosion inhibitors. A Thesis

Submitted to the University of Manchester for the Degree of Doctor of Philosophy 2016:274.
[22] Khaled KF. Studies of iron corrosion inhibition using chemical, electrochemical and computer simulation techniques. Electrochimica Acta 2010;55:6523–32. https://doi.org/10.1016/J.ELECTACTA.2010.06.027.
[23] Xhanari K, Grah N, Finšgar M, Fuchs-Godec R, Maver U. Corrosion inhibition and surface analysis of amines on mild steel in chloride medium. Chemical Papers 2017;71:81–9. https://doi.org/10.1007 /s11696-016-0046-y.
[24] Qian JH, Zhang Y, Yin XY, Liu L. The corrosion inhibitory property of N,N-bis(2-benzimidazolylmethyl)amine for Q235 steel. Materials and Corrosion 2013;64:422–5. https://doi.org/10.1002/maco.201106300.
[25] Elemike EE, Nwankwo HU, Onwudiwe DC. Experimental and theoretical studies of (Z)-N-(2-chlorobenzylidene) naphthalen-1-amine and (Z)-N-(3-nitrobenzylidene)naphthalen-1-amine, and their corrosion inhibition properties. Journal of Molecular Structure 2018;1155:123–32. https://doi.org/10.1016/j.molstruc.2017.10.102.
[26] Abd El-Haleem SM, Abd El-Wanees S. Chloride induced pitting corrosion of nickel in alkaline solutions and its inhibition by organic amines. Materials Chemistry and Physics 2011;128:418–26. https://doi.org/10.1016/ j.matchemphys.2011.03.023.
[27] Goudarzi N, Peikari M, Reza Zahiri M, Reza Mousavi H. Adsorption and corrosion inhibition behavior of stainless steel 316 by aliphatic amine compounds in acidic solution. Archives of Metallurgy and Materials 2012;57:845–51. https://doi.org/10.2478/v10172-012-0044-1.
[28] Abd El Wanees S, Abd El Aal Mohamed A, Abd El Azeem M, El Said R. Inhibition of silver corrosion in nitric acid by some aliphatic amines. Journal of Dispersion Science and Technology 2010;31:1516–25. https://doi.org/10.1080/01932690903294022.
[29] Mahmmod AA, Ismael MH, Fadhil AA, Kurshed NH. Corrosion control of Cu–Ni alloy in hydrochloric acid by amines compounds. International Journal of Corrosion and Scale Inhibition 2019;8:356–65. https://doi.org/10.17675/2305-6894-2019-8-2-15.
[30] Kurmakova, Bondar S, Vorobyova VI, Skiba MI, Tkachenko S V., Makey OP. Peculiarities of the effect of secondary amines with cyclic substituents on microbial steel corrosion. International Journal of Corrosion and Scale Inhibition 2018;7:582–92. https://doi.org/10.17675/2305-6894-2018-7-4-7.
[31] Malinowski S, Wróbel M, Woszuk A. Quantum chemical analysis of the corrosion inhibition potential by aliphatic amines. Materials 2021;14. https://doi.org/10.3390/ma14206197.
[32] Shang W, He C, Wen Y, Wang Y, Zhang Z. Performance evaluation of triethanolamine as corrosion inhibitor for magnesium alloy in 3.5 wt% NaCl solution.RSC Advances2016;6:113967–80.https://doi.org/10.1039/C6RA 23203E.
[33] Palaniappan N, Cole I, Kuznetsov A, Caballero-Briones F, Manickam S. Butylamine functionalized graphene oxide: experimental and DFT studies on the corrosion inhibition efficiency of the MgAZ13 alloy in a 3.5% NaCl environment. Materials Advances 2023:1125–34. https://doi.org/10.1039/d2ma01054b.
[34] Helal NH, Badawy WA. Environmentally safe corrosion inhibition of Mg-Al-Zn alloy in chloride free neutral solutions by amino acids. Electrochimica Acta 2011;56:6581–7. https://doi.org/10.1016/j.electacta.2011.04.031.
[35] Ebenso EE, Alemu H, Umoren SA, Obot IB. Inhibition of mild steel corrosion in sulphuric acid using alizarin yellow GG dye and synergistic iodide additive. International Journal of Electrochemical Science 2008;3:1325–39.
[36] Njong RN, Ndosiri BN, Nfor EN, Offiong OE. Corrosion Inhibitory Studies of Novel Schiff Bases Derived from Hydralazine Hydrochloride on Mild Steel in Acidic Media. Open Journal of Physical Chemistry 2018;08:15–32. https://doi.org/10.4236/ojpc.2018.81002.
[37] Khalifa ORM, Kassab AK, Mohamed HA, Ahmed SY. Corrosion Inhibition of Copper and Copper Alloy in 3M Nitric Acid Solution using Organic Inhibitors. Journal of American Science 2010;6:487–98.
[38] Eddy NO, Ibok UJ, Ebenso EE, Nemr A, El Ashry ESH. Quantum chemical study of the inhibition of the corrosion of mild steel in H2SO4 by some antibiotics. Journal of Molecular Modeling 2009;15:1085–92. https://doi.org/10.1007/ s00894-009-0472-7.
[39] Fiala A, Chibani A, Darchen A, Boulkamh A, Djebbar K. Investigations of the inhibition of copper corrosion in nitric acid solutions by ketene dithioacetal derivatives. Applied Surface Science 2007;253:9347–56. https://doi.org/10.1016/J.APSUSC.2007.05.066.
[40] Philosophy DOF, Kumar P. 18 % Ni M 250 Grade maraging steel under welded condition in acidic 2014.
[41] Fouda AS, Eldesoky AM, El-Sonbati AZ, Salam SF. Prop-2-en-1-one Derivatives as Corrosion Inhibitors for Copper in 1 M HNO3. International Journal of Electrochemical Science 2014;9:1867–91.
[42] Boughoues Y, Benamira M, Messaadia L, Bouider N, Abdelaziz S. Experimental and theoretical investigations of four amine derivatives as effective corrosion inhibitors for mild steel in HCl medium. RSC Advances 2020;10:24145–58. https://doi.org/10.1039/d0ra03560b.
[43] Topal E, Gece G. Untangling the inhibition effects of aliphatic amines on silver corrosion: A computational study. Chemistry Journal of Moldova 2017;12:64–70. https://doi.org/10.19261/cjm.2017.411